HHS Public Access

Author manuscript

Cell Rep. Author manuscript; available in PMC 2017 November 20.

Published in final edited form as:

Cell Rep. 2017 November 14; 21(7): 1896–1909. doi:10.1016/j.celrep.2017.10.078.

Chemotherapy-Induced Depletion of OCT4-Positive Cancer Stem Cells in a Mouse Model of Malignant Testicular Cancer

Timothy M. Pierpont[1], **Amy M. Lyndaker**[1,*,#], **Claire M. Anderson**[1], **Qiming Jin**[1], **Elizabeth S. Moore**[1], **Jamie L. Roden**[1], **Alicia Braxton**[1], **Lina Bagepalli**[1], **Nandita Kataria**[1], **Hilary Zhaoxu Hu**[1], **Jason Garness**[2], **Matthew S. Cook**[2], **Blanche Capel**[2], **Donald H. Schlafer**[1], **Teresa Southard**[1], and **Robert S. Weiss**[1,*,ı]

[1]Department of Biomedical Sciences, College of Veterinary Medicine, Cornell University, Ithaca, NY, USA

[2]Department of Cell Biology, Duke University Medical Center, Durham, NC, USA

Summary

Testicular germ cell tumors (TGCTs) are among the most responsive solid cancers to conventional chemotherapy. To elucidate the underlying mechanisms, we developed a mouse TGCT model featuring germ cell-specific *Kras* activation and *Pten* inactivation. The resulting mice developed malignant, metastatic TGCTs composed of teratoma and embryonal carcinoma, the latter of which exhibited stem cell characteristics, including expression of the pluripotency factor OCT4. Consistent with epidemiological data linking human testicular cancer risk to *in utero* exposures, embryonic germ cells were susceptible to malignant transformation, whereas adult germ cells underwent apoptosis in response to the same oncogenic events. Treatment of tumor-bearing mice with genotoxic chemotherapy not only prolonged survival and reduced tumor size, but selectively eliminated the OCT4-positive cancer stem cells. We conclude that the chemosensitivity of TGCTs derives from the sensitivity of their cancer stem cells to DNA-damaging chemotherapy.

Graphical abstract

[ı]Lead Contact: Robert S. Weiss, Mailing address: T2-006C Veterinary Research Tower, Cornell University, Ithaca, NY 14853, rsw26@cornell.edu, Phone: (607) 253-4443.

[*]Co-corresponding authors

[#]Current address: Division of Mathematics and Natural Sciences, Elmira College, One Park Place, Elmira, NY 14901; alyndaker@elmira.edu

Author Contributions: Conceived and designed the experiments: AML TMP RSW. Performed the experiments: TMP AML CMA QJ ESM JLR AB LB NK HZH. Analyzed the data: TMP AML DHS TS RSW. Contributed reagents/materials/analysis tools: JG MSC BC. Wrote and edited the paper: AML TMP MSC BC RSW.

The authors disclose no potential conflicts of interest.

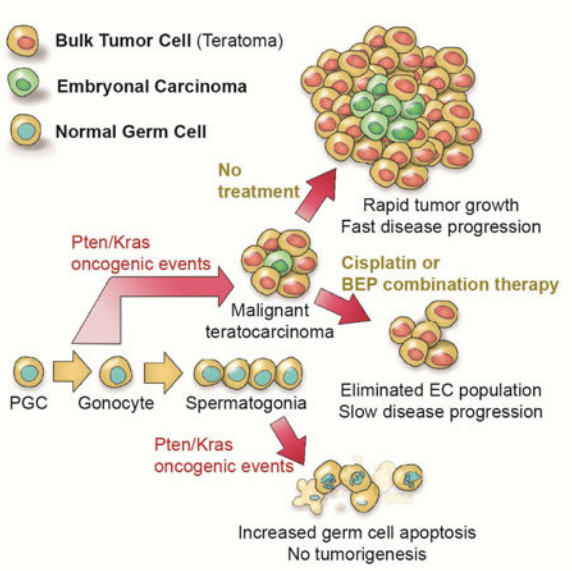

Keywords

Testicular germ cell tumor (TGCT); Cancer stem cells (CSCs); chemotherapy; embryonal carcinoma (EC); DNA damage response (DDR)

Introduction

Testicular germ cell tumors (TGCTs) are the most commonly diagnosed cancers in young men in the U.S. and Europe and are increasing in incidence (Nigam et al., 2014). Intriguingly, testicular cancers are among the most responsive cancers to chemotherapy. Prior to modern genotoxic chemotherapy, the 5-year survival rate for patients diagnosed with metastatic testicular germ cell cancer was only 5%. Remarkably, with conventional chemotherapeutics and surgery, 99% of patients with early-stage disease and 74% of patients with late-stage disease now live at least 5 years (Howlader N, 2016). TGCTs arise from transformed germ cells, most likely prenatal germ cells, such as primordial germ cells or spermatogonial precursors. In the latest classification scheme, TGCTs are categorized by whether or not they originate from a precursor lesion termed germ cell neoplasia in situ (GCNIS) of the testis (Moch et al., 2016). Seminomas and nonseminomas are malignancies that do originate from GCNIS and were referred to as type II TGCTs in earlier classifications. These are the most common TGCTs in adult males and frequently metastasize (Chieffi and Chieffi, 2013). TGCTs that do not originate from GCNIS include infantile teratomas and yolk sac tumors as well as spermatocytic seminomas (previously referred to as type I and type III TGCTs, respectively). To date, mouse TGCT models have featured primarily benign teratomas rather than the more common malignancies originating from GCNIS.

Men presenting with TGCTs often have mixed TGCTs comprised of both seminoma and nonseminoma components, most notably containing highly malignant embryonal carcinoma (EC) tissue. EC cells are totipotent and well established to have stem cell properties. Indeed,

a single EC cell is sufficient to recapitulate an entire tumor (Kleinsmith and Pierce, 1964). EC cells share many characteristics with embryonic stem (ES) cells, and are similarly identified by expression of the pluripotency factor OCT4 (de Jong et al., 2005). OCT4 is used clinically as a diagnostic marker for EC and seminoma as well as early pre-invasive GCNIS lesions (de Jong and Looijenga, 2006). EC cells also express other pluripotency markers, including SOX2 and NANOG (de Jong et al., 2008; Hart et al., 2005), and either differentiate, giving rise to teratoma tissue, or remain undifferentiated and highly malignant, as they do in metastatic TGCTs such as teratocarcinoma, a mixed germ cell tumor composed of EC and teratoma.

Cancer stem cells (CSCs), also referred to as tumor-initiating cells or tumor-propagating cells, are cancer cells with the capacity to self-renew as well as differentiate (Visvader and Lindeman, 2012). Such cell populations have been characterized in several cancers, including glioblastomas, breast cancers, and germ cell tumors. Many somatic CSCs have been linked with chemoresistance, making them particularly interesting clinically because failure to target and eliminate CSCs would leave a patient susceptible to relapse. In contrast to CSCs in somatic cancers, EC cells cultured *in vitro* are sensitive to DNA-damaging chemotherapeutics (Oosterhuis et al., 1984). Furthermore, chemoresistant TGCTs often show loss of pluripotency gene expression (Taylor-Weiner et al., 2016). We propose that the unique chemosensitivity of germ cell-derived CSCs plays an important role in the overall curability of TGCTs and highlights the potential benefit of developing therapies that eliminate CSCs in cancers that are refractory to current treatments.

The molecular basis for the chemosensitivity of TGCTs remains elusive. One explanation for why somatic cancers are resistant to genotoxic chemotherapy is that they accumulate mutations in DNA damage response (DDR) pathways, most notoriously in the *p53* gene (Bartkova et al., 2007b). DDR signals like the early double-strand break marker γH2AX are often constitutively active in early-stage somatic cancers (Bartkova et al., 2005; Bartkova et al., 2007a). This DDR activation can act as a tumorigenesis barrier by slowing or halting cell cycle progression in the presence of oncogene-induced DNA damage, but may also create selective pressure to mutate the genes involved in maintaining that barrier, thus facilitating continued tumorigenesis despite genomic instability (Bartkova et al., 2005; Bartkova et al., 2007a; Bartkova et al., 2007b). Once DDR genes have been mutated, cells no longer respond appropriately to DNA damage, including damage induced by chemotherapy drugs like cisplatin. Depending on the particular genes affected and the tissue context, DDR mutations can either enable avoidance of DNA damage-induced apoptotic signals, conferring chemoresistance, or render cancer cells susceptible to particular genotoxins or to inhibition of residual DDR function, approaches that are now being evaluated for clinical efficacy. Unlike solid tumors of somatic origin, human TGCTs do not exhibit constitutive DDR activation during early tumorigenesis (Bartkova et al., 2007a). This lack of DDR signaling in TGCTs may alleviate the selective pressure to mutate DDR genes, such as *Atm* and *p53*, which are mutated at unusually low frequency in TGCTs compared to somatically derived solid tumors. (Bartkova et al., 2007a; Bartkova et al., 2007b).

Previous studies of malignant TGCTs have focused primarily on analysis of cultured tumor cells and histological sections of human tumors, since genetically engineered mouse models

of TGCT have been limited to those that develop well-differentiated teratomas with little EC and low rates of metastasis, thus being representative of the less-common pediatric TGCTs. These mouse teratoma models include conditional knockout of the *Pten* tumor suppressor targeted to primordial germ cells (Kimura et al., 2003) as well as *129-Dnd1*$^{Ter/Ter}$ mice (Stevens, 1973), which are homozygous for a mutation in the *Dead end* gene (Youngren et al., 2005). Interestingly, the 129 strain background is permissive for testicular teratoma formation in mice; on other strain backgrounds the *Dnd1*$^{Ter/Ter}$ mutation leads to BAX-mediated germ cell apoptosis rather than tumorigenesis (Cook et al., 2009).

Susceptibility genes have been identified for mouse testicular teratomas, including the *Steel* locus, which encodes Kit ligand, as well as additional loci (Bustamante-Marin et al., 2013). Similar susceptibility factors have been identified in human TGCTs, including *PTEN* and *KITLG* (Litchfield et al., 2016). Inactivating *PTEN* mutations in humans specifically mark the transition from TGCT precursor lesions to invasive germ cell tumors (Di Vizio et al., 2005). The most common chromosomal aberration in human TGCTs is isochromosome 12p (Litchfield et al., 2016), an additional copy of a region from the small arm of Chromosome 12 which contains the *KRAS* oncogene (*KRAS2*) as well as several stem cell-related genes (*NANOG, STELLA*, and others).

In order to develop a genetically engineered TGCT mouse model representative of malignant TGCTs in men, we targeted both *Kras* activation and *Pten* tumor suppressor inactivation to pre-meiotic germ cells, which led to rapid development of metastatic mixed testicular germ cell tumors in young male mice. These malignancies contained substantial populations of pluripotent EC cells with tumor-propagating activity, and these cancer stem cells were selectively depleted following chemotherapy, defining a key determinant of the remarkable chemosensitivity of TGCTs.

Results

Generation of germ cell-specific Pten and Kras (gPAK) mutant mice

In order to study the remarkable responsiveness of TGCTs to DNA-damaging chemotherapeutics, we developed a genetically engineered mouse model of malignant, metastatic TGCT by conditionally activating the *Kras* oncogene and inactivating the *Pten* tumor suppressor gene specifically in germ cells. This was accomplished using mice carrying a G12D activating mutation in the first exon of the endogenous *Kras* gene, preceded by a conditional *LoxP-Stop-LoxP* cassette (*LSL-Kras*^{G12D}; (Jackson et al., 2001)), as well as a conditional allele of *Pten* (*Pten*$^{flox/flox}$) in which the critical exon 5 is flanked by *LoxP* sites (Lesche et al., 2002). Recombination between adjacent *LoxP* sites, which enables *Kras*^{G12D} expression and inactivates *Pten*, was mediated by the CRE recombinase under control of a portion of the *Stra8* promoter (*Stra8-Cre*; (Sadate-Ngatchou et al., 2008)), which is active primarily in mitotic spermatogonia in early postnatal life and continuing throughout adulthood. Double mutant experimental animals, which we refer to as gPAK mice for germ cell-specific *Pten* and *Kras* mutant mice, harbored one conditional and one null allele of *Pten* (*Pten*$^{flox/-}$), one copy of the conditional *LSL-Kras*^{G12D} allele (*Kras*$^{+/LSL}$), and the *Stra8-Cre* transgene (*Stra8-Cre*^{Tg}) on a mixed strain background. Both single and double mutant mice were obtained at expected frequencies.

Simultaneous Stra8-Cre-driven Kras activation and Pten inactivation result in testicular germ cell tumorigenesis

While *Kras* activation or *Pten* inactivation individually rarely resulted in TGCT formation, combined *Kras* activation and *Pten* inactivation in gPAK mice led to rapid germ cell tumorigenesis, with 75% of gPAK mice succumbing to large bilateral or unilateral TGCTs with a median tumor-free survival of 24.5 days (Fig. 1A). The reduction in tumor-free survival in gPAK mice as compared to controls was highly significant ($p=1.560\times10^{-6}$), and no control mice developed tumors within the same time period.

TGCTs in these mice were characterized histologically as teratocarcinomas, which are mixed germ cell tumors (nonseminoma) containing teratomatous components, including tissues derived from all three germ layers as well as highly malignant EC tissue (Fig. 1B-F). Metastases that histopathologically resembled the primary neoplasms were detected in at least 37% of TGCT-bearing gPAK mice at various sites, including spleen, liver, pancreas, and abdominal lymph nodes (Fig. 1G).

gPAK TGCTs express OCT4 and other pluripotency markers

The OCT4 transcription factor is a key regulator of pluripotency. OCT4 expression is used in human patients as a diagnostic marker for EC as well as for TGCT precursor lesions (de Jong and Looijenga, 2006). The presence of EC is the main histological feature that distinguishes teratocarcinoma from benign teratoma. To assess OCT4 expression in gPAK TGCTs, we performed OCT4 immunohistochemistry (IHC) on serial sections from early- and late-stage gPAK teratocarcinomas and metastases, as well as on benign *129-Dnd1*$^{Ter/Ter}$ teratomas for comparative purposes. All gPAK tumors contained prominent clusters of OCT4-positive (OCT4^{+}) cells distributed in a multifocal pattern throughout the primary tumors (Fig. 2A-C), as did 50% of metastases (Fig. 2D; proximal lymph node metastasis). In contrast, 3 out of 3 *129-Dnd1*$^{Ter/Ter}$ teratoma samples were OCT4-negative (Fig. 2E). In addition to the use of OCT4 in human TGCT diagnostics, an array of stem cell markers has been established for distinguishing between subtypes of TGCTs. For example, NANOG is a specific marker of EC and seminoma as well as the precursor lesion GCNIS, and is not expressed in mature teratomas (Hart et al., 2005), and SOX2 is expressed in EC but not in GCNIS or seminoma (de Jong et al., 2008). SOX17 is present in GCNIS, seminoma, and teratoma, but not in EC (de Jong et al., 2008; Nonaka, 2009). Similar to what has been reported for human specimens, *129-Dnd1*$^{Ter/Ter}$ teratomas did contain cells expressing SOX2 and SOX17, whereas EC clusters within gPAK teratocarcinomas were positive for the stem cell markers OCT4, NANOG, SSEA1, and SOX2, but were devoid of SOX17 (Fig. 2A,B,E). Thus, gPAK TGCTs express the same stem cell-associated markers as human malignant TGCTs. gPAK TGCTs were also highly proliferative, as indicated by Ki67 staining (Fig. 2B). Finally, we assessed activation of AKT, which is normally opposed by PTEN, in gPAK samples. AKT phosphorylation was observed specifically in tumor tissue from gPAK mice and only in a subset of tumor cells (Fig. 2F).

To determine whether gPAK EC were CSCs, we first tested for tumor propagation by transplantation into secondary recipient mice. Whereas teratomas fail to form secondary tumors upon transplantation (Sachlos et al., 2012), gPAK TGCTs could readily be

transplanted into secondary recipient mice and serially propagated (Table S1), and the resulting tumors contained $OCT4^+$ EC cells (Fig. S1A). These results suggested that EC, the malignant component of teratocarcinoma that is lacking in teratoma, had tumor-propagating activity, in agreement with previous studies (Kleinsmith and Pierce, 1964). To confirm this, we bred an OCT4-GFP transgene into the gPAK model, isolated $OCT4^+$ and $OCT4^-$ cells from the resulting tumors, and tested tumor-propagating activity (Fig. S1B-E). The $OCT4^+$ population formed teratocarcinoma in secondary hosts whereas $OCT4^-$ cells did not, confirming that the $OCT4^+$ EC cells have tumor-propagating activity and function as CSCs.

gPAK TGCTs originate during embryonic development

The rapid development of TGCTs in gPAK mice prompted us to examine the precise timing of tumor initiation in this model. *Stra8* is a developmentally regulated gene that is expressed in early germ cells just prior to their entry into the meiotic program (Feng et al., 2014). In mice, *Stra8* is broadly expressed in spermatogonia beginning at P3. The *Stra8-Cre* transgene, used here to generate gPAK mice, contains a fragment of the *Stra8* promoter that is reported to be expressed in spermatogonial stem cells (Sadate-Ngatchou et al., 2008). While *Stra8-Cre* has been shown to be expressed at P3 in the pre-meiotic spermatogonial cells, we observed substantial tumors, sometimes occupying the majority of the testis, in 3 out of 4 gPAK mice at P10, 1 out of 1 gPAK mouse at P6, and 3 out of 7 gPAK mice at P3, as well as 2 out of 5 *Pten* single mutant mice at P3, suggesting that the neoplasms originate prior to P3 (Fig. 3A). Furthermore, all gPAK mice that developed TGCTs did so by 33 days, suggesting an early developmental window for tumor susceptibility. Thus, in order to determine the precise timing of *Pten/Kras* manipulation in our model, we used a CRE-responsive fluorescent reporter and assessed the precise timing of *Stra8-Cre* activity. While *Stra8-Cre* was broadly expressed in spermatogonia beginning at P3, a few small clusters of *tdTomato*-positive cells (indicative of *Stra8-Cre* expression) were identifiable within the seminiferous tubules beginning at E12.5 and observed in 6 out of 6 embryos (Fig. 3B). No *tdTomato*-positive cells were detected prior to E12.5. From E13.5 to E18.5 the number and approximate size of the clusters remained unchanged. Beginning at P0, additional individual cells throughout the testes became *tdTomato*-positive and the clusters also expanded, resulting in staining throughout the testes by P3. Similar results were observed with a *LacZ* reporter (Fig. S2). The presence of these infrequent clusters of *Cre*-expressing cells in the embryonic testis, together with our observations of only one or two tumor initiation sites per testis in gPAK mice, is consistent with the notion that germ cell tumorigenesis in the gPAK model arises from rare, early *Stra8-Cre* expression in only a few germ cells during embryogenesis. We also used the *tdTomato* reporter in combination with *Pten/Kras* targeting as a sensitive approach to identify early neoplasms and detected well-developed TGCTs in 3 out of 5 gPAK mice at P0 (Fig. 3C), providing further evidence for the *in utero* origins of these neoplasms.

Most pre-invasive somatic cancers express markers of DDR activation, including γH2AX, but human TGCTs interestingly lack such activation (Bartkova et al., 2005; Bartkova et al., 2007a; Bartkova et al., 2007b). It has been proposed that a lack of DDR activation in TGCTs may reduce selective pressure to mutate key DDR genes that enforce the anti-cancer barrier, explaining why TGCTs rarely have mutations in DDR genes like *p53,* unlike somatic

cancers. To test whether gPAK mouse TGCTs similarly share this property, we assessed the presence of γH2AX, one of the earliest DDR signals, in early stage gPAK TGCTs. Similar to the findings in early-stage human TGCTs (Bartkova et al., 2007b), we found that gPAK TGCTs were largely devoid of γH2AX-positive cells, particularly in $OCT4^+$ regions. γH2AX expression was instead confined to the meiotic cells of the seminiferous epithelium, which mount a DDR during normal meiotic progression (Fig. 3D-F). These results provide further parallels between the gPAK TGCT model and human disease, establishing the utility of gPAK mice for investigating the link between DDR activation status and chemosensitivity in these uniquely treatable cancers.

Testicular germ cells exhibit a restricted developmental window of susceptibility to oncogenic transformation

Since *Stra8-Cre* expression occurs early in embryonic testis, and gPAK tumor formation appears to initiate from rare CRE-expressing embryonic germ cells, we were interested in understanding the impact of oncogenic events occurring at higher frequency with the onset of broader CRE expression at P3. Germ cell proliferation and germ cell numbers were therefore quantified in post-natal gPAK mice without apparent neoplasms. We first assessed the cellularity of P3 gPAK testes (Fig. 4A) and performed IHC staining for mouse VASA homolog (MVH/Ddx4; Fig. 4B), which marks early germ cells (Fujiwara et al., 1994). No significant differences in germ cell numbers were detected at P3 in any of the tumor-free single or double mutants (Fig. 4C). There was, however, increased cellularity in the seminiferous epithelium of gPAK testes relative to controls at P10 (81.2 ± 8.8 cells per tubule in gPAK mice versus 56.6 ± 4.1 in controls ($p= 0.0351$)) and P17 (141.5 ± 14.0 cells per tubule in gPAK mice versus 101.4 ± 5.3 in controls ($p= 0.0177$)) (Fig. 4D). To measure proliferating germ cells, we performed IHC staining for the proliferation marker phospho-histone H3 (pH3). Tumor-free gPAK testes had significantly increased numbers of pH3-positive cells at P10 relative to controls ($p=0.045$), but not at P3 (Fig. 4E, F). Interestingly proliferation returned to normal levels by P17 in tumor-free gPAK testes and was followed by dysplastic changes in the testis as early as P30 and P40, accompanied by significantly increased germ cell death ($p<0.005$) (Fig. 5A, 5B, and S3).

By P180 the seminiferous tubules of tumor-free gPAK mice exhibited prominent degenerative changes including vacuolization, pyknotic nuclei, and multinucleate spermatid giant cells as well as increased numbers of TUNEL-positive apoptotic cells apparent at various stages of spermatogenesis (Fig. 5C-E and S3; $p=0.002$). 25% of gPAK mice never developed tumors, and these tumor-free adult gPAK mice had decreased testis size and significantly decreased numbers of epididymal sperm ($p<0.005$ and $p<0.001$, respectively; Fig. 5F,G). *Pten* single mutants showed increased vacuolization and degenerative changes at P180 (Fig. 5C), as well as increased germ cell apoptosis (Fig. 5D,E; $p=0.01$) and significantly reduced sperm counts (Fig. 5G; $p<0.001$). That some gPAK mice experience testicular degeneration rather than tumorigenesis suggests that germ cell transformation in this model likely occurs during a restricted period of embryonic development when male germ cells are susceptible to malignant transformation or when a suitable microenvironment is available to support tumor growth. Subsequent widespread oncogenic events in post-natal germ cells (P3 and beyond) initially promote germ cell hyperproliferation in the postnatal

testis but ultimately lead to germ cell death and impaired fertility rather than malignant transformation and tumorigenesis.

gPAK tumor cells are predominantly diploid and harbor recurrent DNA copy number aberrations

Aneuploidy is a distinguishing characteristic of most cancers. Teratomas, however, have been reported to have normal diploid chromosome numbers (Bussey et al., 1999). To assess chromosomal integrity and also determine whether absence of oncogene-induced DNA damage might underlie the lack of DDR activation seen in human TGCTs (Bartkova et al., 2007a), we performed metaphase chromosome analysis of gPAK teratocarcinoma cells as well as cells from benign 129-*Dnd1*$^{Ter/Ter}$ mouse teratomas. Cells from both tumor types were primarily diploid, with a mean metaphase chromosome number between 38 and 42, indicating that the increased malignancy of gPAK tumors is not associated with gross chromosomal instability (Fig. S4). These results are consistent with findings of near-diploid chromosome numbers in cultured mouse teratocarcinoma cells (Swartzendruber et al., 1976). Thus, if tumorigenesis is associated with oncogene-induced DNA damage in this model, the damage must be comprised of smaller-scale aberrations rather than gross changes in chromosome number or structure.

To further assess oncogene-induced genomic alterations in gPAK tumors, we analyzed copy number aberrations via array comparative genome hybridization (aCGH). As depicted in Fig. S5A and Table S2, gPAK tumors harbored recurrent copy number gains and losses across the six tumors analyzed, including events on Chromosomes 1, 7, 9, 12, 14, 17, and X. A subset of the regions recurrently altered in gPAK tumors were also altered in *129-Dnd1*$^{Ter/Ter}$ tumors (Table S2, right), such as loss of Chr. 7qA3 (Fig. S5B), which was confirmed in both tumor types by qPCR (Fig. S5C). *129-Dnd1*$^{Ter/Ter}$ teratomas additionally harbored recurrent copy number changes on Chromosomes 4, 6, 11, and 20 that were not identified in gPAK tumors (Table S3). Recent genomic analyses of human TGCT revealed a high frequency of copy-neutral reciprocal loss-of-heterozygosity events (Taylor-Weiner et al., 2016), but unfortunately aCGH cannot be used to detect such events. Analysis of the altered gPAK chromosomal regions via Panther and Enrichr gene list analysis tools revealed enrichment for G-protein-coupled receptors ($p=3.45\times10^{-21}$) and receptors ($p=1.79\times10^{-11}$) as well as for genes regulated by particular transcription factors, most notably SOX2 (33/188 genes, $p=4.97\times10^{-18}$; Table S4). SOX2 is highly expressed in gPAK neoplasms, likely reflecting the cell of origin and consistent with the idea that regions of the genome containing highly expressed gene clusters are prone to replication-associated chromosome breakage (Barlow et al., 2013).

gPAK TGCTs are sensitive to chemotherapy

TGCTs in humans are exquisitely sensitive to the DNA-damaging chemotherapeutic cisplatin, which is used routinely as a frontline drug in combination with bleomycin and etoposide. To determine whether gPAK TGCTs were also chemosensitive, gPAK mice were treated intraperitoneally with either two 6 mg/kg cisplatin doses, or a full course of bleomycin/etoposide/cisplatin (BEP) at doses comparable to those used in humans. Cisplatin-treated gPAK mice lived significantly longer than untreated gPAK mice

(p=0.0192), with a median survival of 36 days for untreated mice and 49 days for cisplatin-treated mice (Fig. 6A). Two cisplatin doses were not sufficient to eradicate the tumors, and treated mice ultimately reached humane endpoint criteria; however, primary tumor volume at endpoint was significantly lower in cisplatin-treated gPAK mice than in untreated animals (p=0.004; Fig. 6B). gPAK mice were even more responsive to BEP, with several mice surviving to an arbitrary 100 day end point (median survival of 87.5 days; p<0.001) and primary tumor volume significantly reduced (p=0.002). Thus, gPAK murine TGCTs, similar to their human counterparts, can be effectively treated with chemotherapy, even in the absence of the surgical interventions that typically accompany chemotherapy in humans.

gPAK CSCs are significantly depleted following genotoxic chemotherapy

To directly test how EC cells respond to chemotherapy *in vivo,* we quantified OCT4-expressing cells in gPAK tumors collected at endpoint from mice treated with cisplatin or BEP. Strikingly, the percentage of $OCT4^+$ cells was significantly reduced in the gPAK mice treated with either cisplatin alone or BEP (Fig. 6C,D; p=0.02 and p=0.01 respectively). To understand how the chemosensitivity of $OCT4^+$ EC cells compared with that of bulk tumor cells, we also stained for SOX17, which is present in a subset of non-EC tumor cells. The percentage of SOX17-positive cells within gPAK TGCTs was not decreased in response to BEP or cisplatin treatment, in contrast to what we observed for $OCT4^+$ EC cells (Fig. S6 and Fig. 6E). We conclude that TGCT chemosensitivity is specifically linked to the responsiveness of EC cells to genotoxic chemotherapy. Since EC cells are the CSCs of TGCTs, this selective sensitivity may explain why chemotherapy in humans is more effective against TGCTs than somatic solid cancers.

In order to understand the acute responses to chemotherapy in gPAK TGCTs, tumor-bearing gPAK mice were euthanized at 12 or 48 hours after a single dose of 6 mg/kg cisplatin Apoptosis was significantly increased at 12 hours post-treatment (4.5 ± 1.2 (treated) vs. 0.67 ± 0.5 (untreated) apoptotic cells per field, p=0.0378) (Fig. 7A). Apoptosis appeared to be enriched within $OCT4^+$ clusters and by 48 hours nearly all $OCT4^+$ cell clusters exhibited altered morphology and reduced cell number. Importantly, this indicates that the $OCT4^+$ EC cells in gPAK TGCTs are sensitive to cisplatin-induced DNA damage, which leads to rapid initiation of apoptosis and elimination of CSCs. Consistent with this notion, γ-H2AX staining was clearly increased in gPAK tumors at 6 hours post-cisplatin treatment (Fig. 7B).

Following chemotherapy, surviving CSCs that are refractory to treatment can cause tumor recurrence. To determine whether the reduced amount of EC in gPAK tumors post-treatment correlated with reduced tumor-propagating activity, we compared tumor formation following transplantation of tumor cells from treated or untreated gPAK mice. Subcutaneous injection of 10,000 cells from untreated gPAK TGCTs was sufficient to produce tumors at 75% of injection sites (n=16; Fig. 7C and Table S5). By contrast, 25,000 gPAK tumor cells transplanted 48 hours post-cisplatin treatment failed to result in tumor formation in recipient mice (n=20). Tumor-propagating activity was not completely eradicated by cisplatin treatment, as transplantation of 1 million or 100,000 cells from treated gPAK tumors was sufficient for tumor formation, though with much longer latency than observed for untreated tumor cells (p<0.005). Limiting dilution calculations based on these data estimated a

frequency of viable CSCs of 1 in 9167 tumor cells from untreated gPAK TGCTs, which likely underestimates the true frequency of the CSCs due to EC cell death during tumor disaggregation (Table S5). Notably, cisplatin-treated gPAK TGCTs contained only 1 CSC in 252,332 tumor cells, signifying a 28-fold reduction in CSC frequency following treatment. Since a single intact EC cell is sufficient to induce tumorigenesis (Kleinsmith and Pierce, 1964), these results support the notion that the chemosensitivity of TGCT CSCs underlies the remarkable curability of TGCTs. Consistent with this conclusion, $OCT4^{+}$ EC cells were detected in 4/5 tumors arising from transplants derived from untreated mice, but none of 4 tumors formed by cells from cisplatin-treated animals (Table S5).

Discussion

In this study, we developed a mouse model of malignant TGCT that, like human TGCTs, exhibits marked chemosensitivity that is associated with an inherent sensitivity of EC cells, the CSCs of TGCT, to elimination by conventional genotoxic chemotherapy. This is in contrast to most CSCs, which are refractory to treatment and often contribute to disease recurrence following initial chemotherapeutic treatment (Visvader and Lindeman, 2012). This establishes a powerful system for testing the molecular mechanism underlying the chemosensitivity of these unique CSCs, which we hypothesize is a direct consequence of germ cells having a distinct DDR compared to other cell types. Since there are several known determinants of cisplatin sensitivity, including DNA repair factors, studies of their roles in EC cells may reveal strategies for sensitizing other types of cancers with chemoresistant CSCs. The apparent proliferative state of gPAK CSCs may also contribute to their chemosensitivity, as quiescence may help CSCs in other tumors survive genotoxic therapies. Finally, EC cells may be poised to undergo damage-induced apoptosis due to mitochondrial priming, which has been observed in human TGCTs (Taylor-Weiner et al., 2016).

We observed tumors in gPAK mice at birth (P0), indicating that the tumors most likely do not arise from postnatal initiation events but rather from rare transformation of embryonic germ cells. Consistent with this, we were able to detect *Stra8-Cre*-mediated recombination in a few small clusters of testicular germ cells at E12.5 and subsequently observed only 1-2 neoplasms per testis. It remains unknown whether the embryonic *Cre* expression observed in this model reflects the normal activity of the *Stra8* promoter or is unique to the *Stra8-Cre* transgene. Male germ cells show endogenous *Stra8* mRNA expression at E13.5 (Heaney et al., 2012) and a small subset of male germ cells express meiotic markers at E14.5 (Yao et al., 2003), suggesting that *Stra8* expression can occur naturally during embryonic germ cell development. Regardless, the data suggest that gPAK TGCT initiation occurs in early/mid-embryonic germ cells, a time point between PGC arrival at the gonad and the onset of G0 cell cycle arrest (Bustamante-Marin et al., 2013). Notably, teratoma formation in Dnd^{Ter} mice is associated with a failure of embryonic germ cells to undergo proper mitotic arrest, suggesting that G0 arrest and downregulation of pluripotency gene expression at E12.5 to E15.5 may mark the end of the period during which germ cells are particularly susceptible to malignant transformation (Cook et al., 2011). Interestingly, *Kras* and *Pten* targeting in postnatal germ cells initially triggered widespread overproliferation but ultimately led to cell death and germ cell depletion. Together, our results suggest that there is a specific

developmental window during which TGCTs can arise (Fig. S7). This mimics the case in humans, where epidemiologic data indicate that TGCT risk in men is associated with *in utero* environmental exposures (McGlynn and Cook, 2009). It may be that the microenvironment in post-natal testes is not conducive to tumor initiation or that molecular features of germ cells protect against oncogenic events in adults but allow sustained hyperproliferation at certain stages of embryogenesis. Interestingly, loss of the pro-apoptotic gene *Bax* causes testis hypercellularity soon after birth, followed by massive cell death at P25, suggesting the existence of mechanisms to eliminate excess germ cells from adult testes (Russell et al., 2002).

It is unclear why *Kras* activation or *Pten* inactivation alone is insufficient to cause germ cell tumorigenesis in the majority of cases. It has been reported previously that *Stra8-Cre*-driven *Pten* loss does not induce TGCTs or affect fertility (Huang et al., 2011), although in our studies we did see infrequent TGCTs as well as germ cell loss with *Pten* deletion alone, perhaps reflecting differences in mouse strain background in these studies. No TGCTs were observed in mice with *Stra8-Cre*-driven *Kras* activation alone even after one year. That *Ras* activation is insufficient for oncogenic transformation in germ cells is consistent with reports that some mouse tissues are more susceptible to *Ras*-induced transformation than others. Mice expressing activated oncogenic *Kras* in somatic tissues primarily develop lung cancers as well as oral, gastric, and skin papillomas and thymic lymphomas, but rarely neoplasms of other tissue origins (Guerra et al.; Johnson et al., 2001). Substantial evidence indicates that *Pten* loss and *Kras* activation can be potent collaborating events during tumorigenesis, including in ovarian cancer (Mullany et al., 2011), pancreatic cancer (Hill et al., 2010), and melanoma (Nogueira et al., 2010). Thus, *Pten* loss and *Kras* activation are functionally non-equivalent, despite their overlapping impact on key signaling pathways, and in the context of germ cells strongly synergize to promote TGCT formation.

The contrasting effects of *Pten* and *Kras* alterations in germ cells may be particularly relevant to their modulation of the germline stem cell pool. *Pten* inactivation in oocytes promotes premature activation of the entire primordial follicle pool, causing an initial surge of follicle maturation that leads to premature ovarian failure (Reddy et al., 2008). *Ras* activation in cultured spermatogonial stem cells (SSCs), on the other hand, promotes proliferation and self-renewal rather than differentiation (Lee et al., 2009). Interestingly, excessive self-renewal triggered by activated *Hras* in cultured SSCs led to germ cell tumors upon transplantation into murine testes. It is possible that the combined *Pten* inactivation and *Kras* activation in our model promotes premature cell division of SSC precursors concomitant with activation of excessive self-renewal signals, leading to development of germ cell-derived tumors containing $OCT4^{+}$ malignant stem cells (EC cells). Supporting this idea is the fact that *Pten* null mouse pluripotent stem cells cultured *in vitro* develop into aggressive, tumorigenic EC cells through increased survival and self-renewal caused by loss of *Nanog* repression (Lindgren et al., 2011).

Many questions remain regarding TGCT biology, most notably related to the fundamental differences in the cell of origin between germ cell and somatically-derived cancers and the different molecular mechanisms governing their responses to oncogenic transformation. In stark contrast to most somatically-derived cancers, early-stage TGCTs in our gPAK mice

and humans (Bartkova et al., 2007b) lack markers of DDR activation such as γH2AX, despite the fact that TGCTs can mount a robust DDR to genotoxic chemotherapy. This fundamental difference in response to oncogene-induced DNA damage may be due to differential DDR wiring of germ cells *versus* somatic cells or dampening of the DDR in pre-meiotic germ cells to allow full DDR activation following meiotic DSB induction, which is absolutely necessary for completion of meiosis and production of functional sperm. It remains to be seen whether germ cells in fact incur as much DNA damage in response to oncogenic proliferation as do somatic cells, which would also impact DDR activation. Interestingly, ES cells contain greater numbers of dormant origins than more differentiated cells (Ge et al., 2015), and it is conceivable that embryonic germ cells could use this or related mechanisms to protect against replication stress that normally accompanies oncogene-induced hyperproliferation. Whether the DDR is differentially regulated depending on germ cell developmental stage also remains to be determined. For instance, whereas embryonic germ cells do not appear to mount a DDR against oncogenic events, the germ cell apoptosis associated with oncogenic events in adult gPAK mice could reflect a DDR triggered by replication stress associated with the widespread hyperproliferation observed at P10. Identification of the molecular features that make TGCT CSCs so sensitive to DNA-damaging chemotherapeutics may yield broadly applicable biomarkers for chemo-sensitivity or -resistance and provide avenues for the development of more effective therapies for other cancers by targeting their more deadly, chemoresistant CSCs.

Experimental Procedures

Mouse strains and husbandry

All animals used in this study were handled in accordance with federal and institutional guidelines, under a protocol approved by the Cornell University Institutional Animal Care and Use Committee. Male mice of up to 6 months in age were used for analysis of TGCT formation. The following strains, with strain backgrounds in parentheses, were used: *Stra8-Cre* (129S6); LSL-Kras^{G12D} (129S6); Pten^{flox} (mixed C57BL/6J, 129S6, FVB); *Tg(Pou5f1-EGFP)2Mnn* (mixed C57BL/6J, 129S6); *Gt(ROSA)26Sor^{tm1Sor}* (C57BL/6J); *Gt(ROSA)26Sor$^{tm9(CAG-tdTomato)Hze}$* (C57BL/6J); *Dnd1^{Ter}* (129X1). Please refer to the Supplemental Experimental Procedures for additional details about strains used and breeding strategies.

Histology and immunohistochemistry

IHC staining for OCT4, γH2AX, SOX17, SOX2, MVH, Ki67, SSEA1, Nanog, and phospho-AKT was performed as described in the Supplemental Experimental Procedures. TUNEL assays were performed using the Apoptag kit (Millipore) as per the manufacturer's instructions.

Lineage tracing with LacZ and tdTomato reporters

LacZ staining and tdTomato analysis of testes was performed as described in the Supplemental Experimental Procedures.

Metaphase chromosome analysis

Metaphase chromosome spreads were prepared from gPAK or *129-Dnd1*$^{Ter/Ter}$ testicular tumor cells (three primary tumors per genotype) as described in the Supplemental Experimental Procedures.

Array comparative genome hybridization (CGH)

Six tumors each from gPAK or *129-Dnd1*$^{Ter/Ter}$ were analyzed using NimbleGen Mouse CGH 3×720k Whole Genome Tiling Arrays (Roche) as described in the Supplemental Experimental Procedures. Partial karyotype depiction of gPAK copy number aberration data (Fig. S5A) was generated using waviCGH. Validation of 7qA3 deletion in gPAK and *129-Dnd1*$^{Ter/Ter}$ tumors was performed by qPCR.

Chemotherapy treatments

Treatment of mice with Cisplatin (Sigma P-4394) alone, or a combination of Cisplatin, Bleomycin (Selleckchem), and Etoposide (Selleckchem) were performed as described in the Supplemental Experimental Procedures.

gPAK TGCT transplantation

Transplantations of gPAK TGCT cells into secondary hosts were performed as described in the Supplemental Experimental Procedures. Mice were monitored regularly for tumor development and sacrificed upon reaching humane endpoint criteria.

Statistical Analyses

Statistical tests were done using Prism (GraphPad Software, La Jolla CA, USA), R (v.3.3.1; the R Foundation for Statistical Computing; http://www.r-project.org/), or Excel (Microsoft). Specific tests, P-values, and sample size are reported in the figure legends or text with appropriate data.

Supplementary Material

Refer to Web version on PubMed Central for supplementary material.

Acknowledgments

The authors are grateful to Drs. Peter Schweitzer and Wei Wang of the Cornell University Genomics Core Facility for aCGH analysis; Lishuang Shen and Marsha Wallace for assistance with CGH and qPCR; Drs. Robert Braun, Alexander Nikitin, and Doina Tumbar for providing mice; and Alex Nikitin and Andrew White for comments on the manuscript. This work was supported by the Cornell University Center for Vertebrate Genomics (microarray subsidy), NIH T32 HD052471 training grant support to AML, NIH T32 GM07273 training grant support to TP and LB, NIH T32 ODO011000 training grant support to ESM, NIH R01 GM087500 to BC, NIH T35 AI007227 training grant support to AB, NK, and HZ, NYSTEM IDEA award C026421 to RSW, and NIH R21 CA185256 to RSW.

References

Barlow JH, Faryabi RB, Callen E, Wong N, Malhowski A, Chen HT, Gutierrez-Cruz G, Sun HW, McKinnon P, Wright G, et al. Identification of early replicating fragile sites that contribute to genome instability. Cell. 2013; 152:620–632. [PubMed: 23352430]

Bartkova J, Horejsi Z, Koed K, Kramer A, Tort F, Zieger K, Guldberg P, Sehested M, Nesland JM, Lukas C, et al. DNA damage response as a candidate anti-cancer barrier in early human tumorigenesis. Nature. 2005; 434:864–870. [PubMed: 15829956]

Bartkova J, Horejsi Z, Sehested M, Nesland JM, Rajpert-De Meyts E, Skakkebak NE, Stucki M, Jackson S, Lukas J, Bartek J. DNA damage response mediators MDC1 and 53BP1: constitutive activation and aberrant loss in breast and lung cancer, but not in testicular germ cell tumours. Oncogene. 2007a; 26:7414–7422. [PubMed: 17546051]

Bartkova J, Rajpert-De Meyts E, Skakkebæk NE, Lukas J, Bartek J. DNA damage response in human testes and testicular germ cell tumours: biology and implications for therapy. Int J Andrology. 2007b; 30:282–291.

Bussey KJ, Lawce HJ, Olson SB, Arthur DC, Kalousek DK, Krailo M, Giller R, Heifetz S, Womer R, Magenis RE. Chromosome abnormalities of eighty-one pediatric germ cell tumors: sex-, age-, site-, and histopathology-related differences--a Children's Cancer Group study. Genes Chromosom Canc. 1999; 25:134–146.

Bustamante-Marin X, Garness JA, Capel B. Testicular teratomas: an intersection of pluripotency, differentiation and cancer biology. Int J Dev Biol. 2013; 57:201–210. [PubMed: 23784831]

Chieffi P, Chieffi S. Molecular biomarkers as potential targets for therapeutic strategies in human testicular germ cell tumors: An overview. J Cell Phys. 2013; 228:1641–1646.

Cook MS, Coveney D, Batchvarov I, Nadeau JH, Capel B. BAX-mediated cell death affects early germ cell loss and incidence of testicular teratomas in Dnd1Ter/Ter mice. Dev Biol. 2009; 328:377–383. [PubMed: 19389346]

Cook MS, Munger SC, Nadeau JH, Capel B. Regulation of male germ cell cycle arrest and differentiation by DND1 is modulated by genetic background. Development. 2011; 138:23–32. [PubMed: 21115610]

de Jong J, Looijenga LH. Stem cell marker OCT3/4 in tumor biology and germ cell tumor diagnostics: history and future. Crit rev oncogenesis. 2006; 12:171–203. [PubMed: 17425502]

de Jong J, Stoop H, Dohle GR, Bangma CH, Kliffen M, van Esser JW, van den Bent M, Kros JM, Oosterhuis JW, Looijenga LH. Diagnostic value of OCT3/4 for pre-invasive and invasive testicular germ cell tumours. J pathol. 2005; 206:242–249. [PubMed: 15818593]

de Jong J, Stoop H, Gillis AJ, van Gurp RJ, van de Geijn GJ, Boer M, Hersmus R, Saunders PT, Anderson RA, Oosterhuis JW, Looijenga LH. Differential expression of SOX17 and SOX2 in germ cells and stem cells has biological and clinical implications. J pathol. 2008; 215:21–30. [PubMed: 18348160]

Di Vizio D, Cito L, Boccia A, Chieffi P, Insabato L, Pettinato G, Motti ML, Schepis F, D'Amico W, Fabiani F, et al. Loss of the tumor suppressor gene PTEN marks the transition from intratubular germ cell neoplasias (ITGCN) to invasive germ cell tumors. Oncogene. 2005; 24:1882–1894. [PubMed: 15674339]

Feng CW, Bowles J, Koopman P. Control of mammalian germ cell entry into meiosis. Mol Cell Endocrinol. 2014; 382:488–497. [PubMed: 24076097]

Fujiwara Y, Komiya T, Kawabata H, Sato M, Fujimoto H, Furusawa M, Noce T. Isolation of a DEAD-family protein gene that encodes a murine homolog of Drosophila vasa and its specific expression in germ cell lineage. PNAS. 1994; 91:12258–12262. [PubMed: 7991615]

Ge XQ, Han J, Cheng EC, Yamaguchi S, Shima N, Thomas JL, Lin H. Embryonic Stem Cells License a High Level of Dormant Origins to Protect the Genome against Replication Stress. Stem cell rep. 2015; 5:185–194.

Guerra C, Mijimolle N, Dhawahir A, Dubus P, Barradas M, Serrano M, Campuzano V, Barbacid M. Tumor induction by an endogenous K-ras oncogene is highly dependent on cellular context. Cancer Cell. 2003; 4:111–120. [PubMed: 12957286]

Hart AH, Hartley L, Parker K, Ibrahim M, Looijenga LH, Pauchnik M, Chow CW, Robb L. The pluripotency homeobox gene NANOG is expressed in human germ cell tumors. Cancer. 2005; 104:2092–2098. [PubMed: 16206293]

Heaney JD, Anderson EL, Michelson MV, Zechel JL, Conrad PA, Page DC, Nadeau JH. Germ cell pluripotency, premature differentiation and susceptibility to testicular teratomas in mice. Development. 2012; 139:1577–1586. [PubMed: 22438569]

Hill R, Calvopina JH, Kim C, Wang Y, Dawson DW, Donahue TR, Dry S, Wu H. PTEN loss accelerates KrasG12D-induced pancreatic cancer development. Cancer Res. 2010; 70:7114–7124. [PubMed: 20807812]

Howlader, N.N, A.Krapcho, M.Miller, D.Bishop, K.Altekruse, SF.Kosary, CL.Yu, M.Ruhl, J.Tatalovich, Z.Mariotto, A.Lewis, DR.Chen, HS.Feuer, EJ., Cronin, KA., editors. SEER Cancer Statistics Review, 1975-2013. NCI; Bethesda, MD: 2016.

Huang Y, Mao X, Boyce T, Zhu GZ. Dispensable role of PTEN in mouse spermatogenesis. Cell Biol Int. 2011; 35:905–908. [PubMed: 21524277]

Jackson EL, Willis N, Mercer K, Bronson RT, Crowley D, Montoya R, Jacks T, Tuveson DA. Analysis of lung tumor initiation and progression using conditional expression of oncogenic K-ras. Genes Dev. 2001; 15:3243–3248. [PubMed: 11751630]

Johnson L, Mercer K, Greenbaum D, Bronson RT, Crowley D, Tuveson DA, Jacks T. Somatic activation of the K-ras oncogene causes early onset lung cancer in mice. Nature. 2001; 410:1111–1116. [PubMed: 11323676]

Kimura T, Suzuki A, Fujita Y, Yomogida K, Lomeli H, Asada N, Ikeuchi M, Nagy A, Mak TW, Nakano T. Conditional loss of PTEN leads to testicular teratoma and enhances embryonic germ cell production. Development. 2003; 130:1691–1700. [PubMed: 12620992]

Kleinsmith LJ, Pierce GB Jr. Multipotentiality of Single Embryonal Carcinoma Cells. Cancer Res. 1964; 24:1544–1551. [PubMed: 14234000]

Lee J, Kanatsu-Shinohara M, Morimoto H, Kazuki Y, Takashima S, Oshimura M, Toyokuni S, Shinohara T. Genetic reconstruction of mouse spermatogonial stem cell self-renewal in vitro by Ras-cyclin D2 activation. Cell Stem Cell. 2009; 5:76–86. [PubMed: 19570516]

Lesche R, Groszer M, Gao J, Wang Y, Messing A, Sun H, Liu X, Wu H. Cre/loxP-mediated inactivation of the murine Pten tumor suppressor gene. Genesis. 2002; 32:148–149. [PubMed: 11857804]

Lindgren AG, Natsuhara K, Tian E, Vincent JJ, Li X, Jiao J, Wu H, Banerjee U, Clark AT. Loss of Pten causes tumor initiation following differentiation of murine pluripotent stem cells due to failed repression of Nanog. PLoS One. 2011; 6:e16478. [PubMed: 21304588]

Litchfield K, Levy M, Huddart RA, Shipley J, Turnbull C. The genomic landscape of testicular germ cell tumours: from susceptibility to treatment. Nat Rev Urol. 2016; 13:409–419. [PubMed: 27296647]

McGlynn KA, Cook MB. Etiologic factors in testicular germ cell tumors. Future oncol. 2009; 5:1389–1402. [PubMed: 19903067]

Moch H, Cubilla AL, Humphrey PA, Reuter VE, Ulbright TM. The 2016 WHO Classification of Tumours of the Urinary System and Male Genital Organs-Part A: Renal, Penile, and Testicular Tumours. Eur Urol. 2016; 70:93–105. [PubMed: 26935559]

Mullany LK, Fan HY, Liu Z, White LD, Marshall A, Gunaratne P, Anderson ML, Creighton CJ, Xin L, Deavers M, et al. Molecular and functional characteristics of ovarian surface epithelial cells transformed by KrasG12D and loss of Pten in a mouse model in vivo. Oncogene. 2011; 30:3522–3536. [PubMed: 21423204]

Nigam M, Aschebrook-Kilfoy B, Shikanov S, Eggener S. Increasing incidence of testicular cancer in the United States and Europe between 1992 and 2009. World J Urol. 2014:1–9.

Nogueira C, Kim KH, Sung H, Paraiso KH, Dannenberg JH, Bosenberg M, Chin L, Kim M. Cooperative interactions of PTEN deficiency and RAS activation in melanoma metastasis. Oncogene. 2010; 29:6222–6232. [PubMed: 20711233]

Nonaka D. Differential Expression of SOX2 and SOX17 in Testicular Germ Cell Tumors. Am J Clin Pathol. 2009; 131:731–736. [PubMed: 19369635]

Oosterhuis JW, Andrews PW, Knowles BB, Damjanov I. Effects of cis-platinum on embryonal carcinoma cell lines in vitro. Int J canc. 1984; 34:133–139.

Reddy P, Liu L, Adhikari D, Jagarlamudi K, Rajareddy S, Shen Y, Du C, Tang W, Hamalainen T, Peng SL, et al. Oocyte-specific deletion of Pten causes premature activation of the primordial follicle pool. Science. 2008; 319:611–613. [PubMed: 18239123]

Russell LD, Chiarini-Garcia H, Korsmeyer SJ, Knudson CM. Bax-dependent spermatogonia apoptosis is required for testicular development and spermatogenesis. Biol reprod. 2002; 66:950–958. [PubMed: 11906913]

Sachlos E, Risueno RM, Laronde S, Shapovalova Z, Lee JH, Russell J, Malig M, McNicol JD, Fiebig-Comyn A, Graham M, et al. Identification of drugs including a dopamine receptor antagonist that selectively target cancer stem cells. Cell. 2012; 149:1284–1297. [PubMed: 22632761]

Sadate-Ngatchou PI, Payne CJ, Dearth AT, Braun RE. Cre recombinase activity specific to postnatal, premeiotic male germ cells in transgenic mice. Genesis. 2008; 46:738–742. [PubMed: 18850594]

Stevens L. A new inbred subline of mice (129-terSv) with a high incidence of spontaneous congenital testicular teratomas. J Natl Cancer Inst. 1973; 50:235–242. [PubMed: 4692863]

Swartzendruber DE, Cram LS, Lehman JM. Microfluorometric analysis of DNA content changes in a murine teratocarcinoma. Cancer Res. 1976; 36:1894–1899. [PubMed: 944615]

Taylor-Weiner A, Zack T, O'Donnell E, Guerriero JL, Bernard B, Reddy A, Han GC, AlDubayan S, Amin-Mansour A, Schumacher SE, et al. Genomic evolution and chemoresistance in germ-cell tumours. Nature. 2016; 540:114–118. [PubMed: 27905446]

Visvader JE, Lindeman GJ. Cancer stem cells: current status and evolving complexities. Cell Stem Cell. 2012; 10:717–728. [PubMed: 22704512]

Yao HH, DiNapoli L, Capel B. Meiotic germ cells antagonize mesonephric cell migration and testis cord formation in mouse gonads. Development. 2003; 130:5895–5902. [PubMed: 14561636]

Youngren KK, Coveney D, Peng X, Bhattacharya C, Schmidt LS, Nickerson ML, Lamb BT, Deng JM, Behringer RR, Capel B, et al. The Ter mutation in the dead end gene causes germ cell loss and testicular germ cell tumours. Nature. 2005; 435:360–364. [PubMed: 15902260]

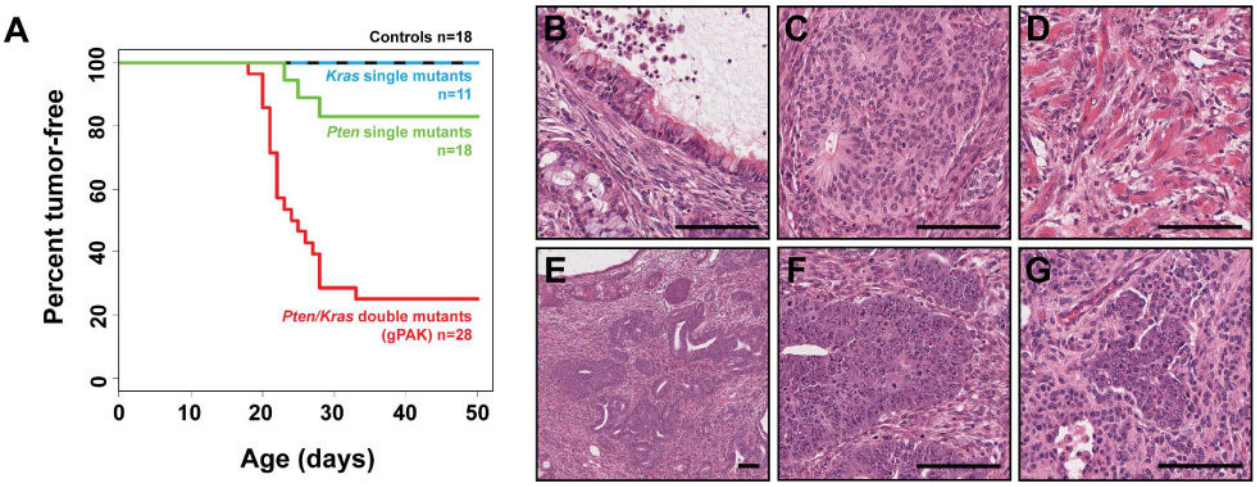

Figure 1. Combined *Pten* and *Kras*^{G12D} targeting in early germ cells results in rapid testicular tumorigenesis

A. Kaplan-Meier tumor-free survival curve depicting that 75% of *Stra8-Cre*^{Tg} *Pten*$^{flox/-}$ *Kras*$^{+/LSL}$ (*Pten/Kras* double mutant, or gPAK) mice and 17% of *Stra8-Cre*^{Tg} *Pten*$^{flox/-}$ *Kras*$^{+/+}$ (*Pten* single mutant) mice developed palpable testicular cancers by 4 weeks of age. No tumors developed in *Stra8-Cre*^{Tg} *Pten*$^{+/flox}$ *Kras*$^{+/LSL}$ (*Kras* single mutant) or control mice (including *Cre*-negative as well as *Stra8-Cre*^{Tg} *Pten*$^{+/flox}$ *Kras*$^{+/+}$ animals). Tumor-free survival was significantly reduced in gPAK mice relative to controls (log rank test; $p=1.56\times10^{-6}$), but not in *Pten* single mutants despite low incidence tumor formation (log rank test; p=0.0713). B-D. High magnification images of differentiated tissues within gPAK TGCTs indicative of teratomatous components, including: respiratory epithelium (B; endoderm), neural cells (C; ectoderm), and skeletal muscle (D; mesoderm). E,F. Low (E) and high (F) magnification images of EC within a teratocarcinoma. G. EC present in a lumbar lymph node metastasis. Scale bars represent 100 μm.

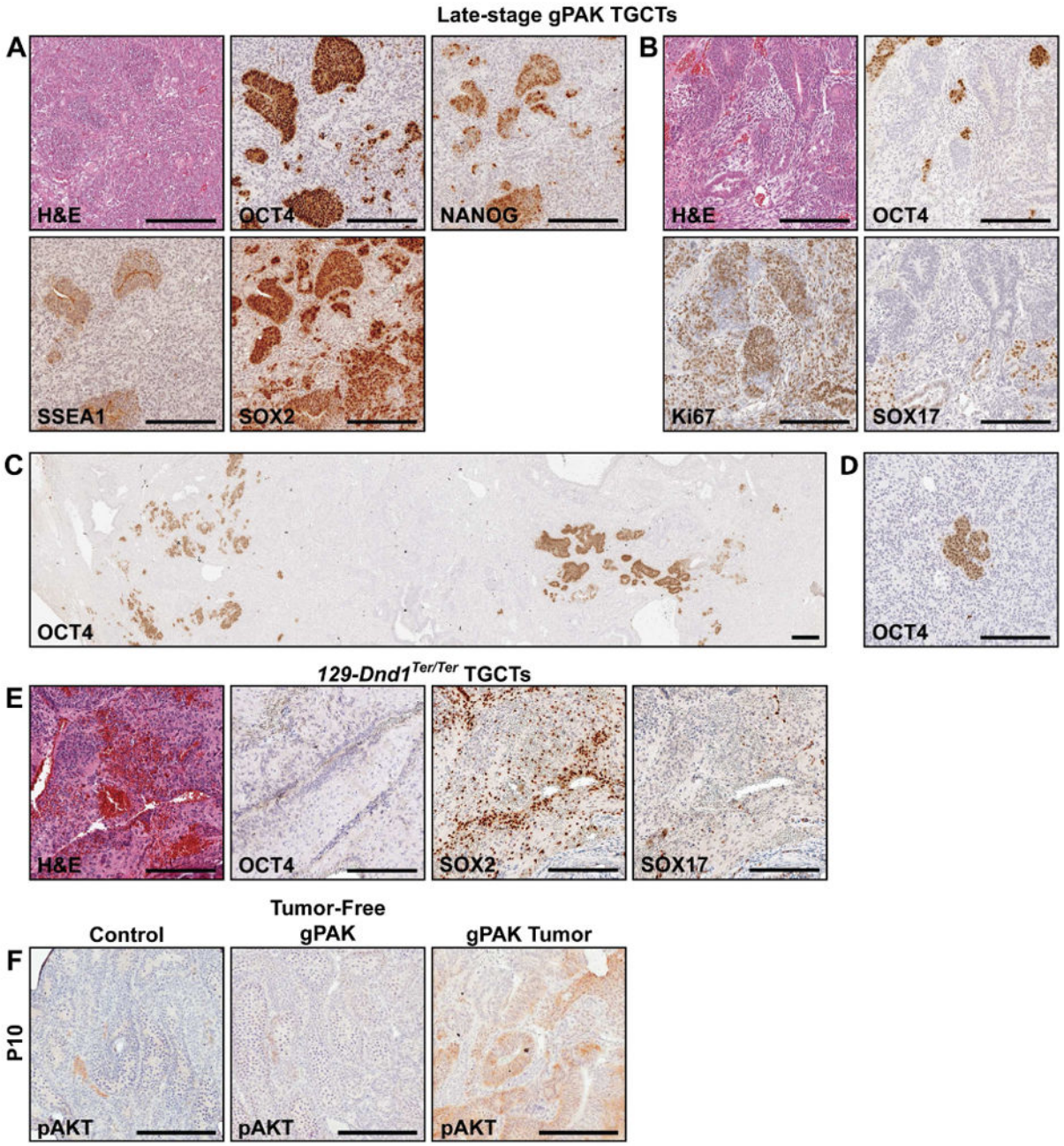

Figure 2. gPAK testicular germ cell tumors contain OCT4^{+} cell clusters that express pluripotency markers but not SOX17

IHC staining for stem cell and proliferation markers of gPAK tumors (A-D, F) and *129-Dnd1$^{Ter/Ter}$* tumors (E). A. OCT4^{+} cells in gPAK TGCTs are also positive for NANOG, SSEA1, and SOX2. B. OCT4^{+} regions of gPAK TGCTs are distinct from those expressing SOX17 and include proliferating, Ki67-positive cells. C. Low magnification view of OCT4^{+} cell distribution in a primary gPAK TGCT. D. OCT4^{+} EC within a proximal lymph node metastasis (see Fig. 1G for H&E image). E. Lack of OCT4 expression in *129-Dnd$^{Ter/Ter}$* teratomas, which express SOX2 and SOX17. Scale bars represent 200 μm. F. Staining for

phospho-AKT in testes from p10 mice revealed AKT activation in gPAK tumors but not in normal control or tumor-free gPAK tubules. Scale bars represent 200 μm.

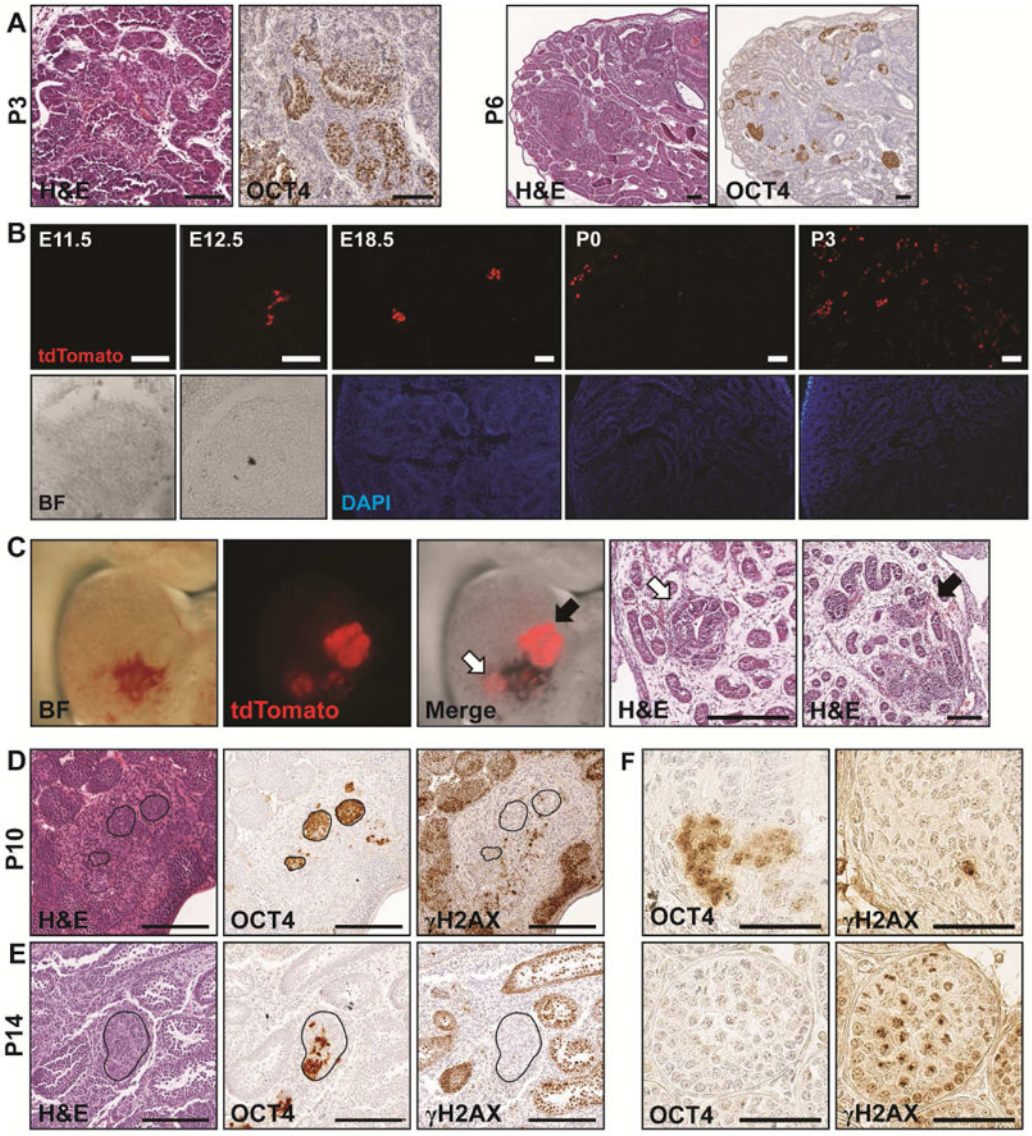

Figure 3. gPAK testicular tumors initiate during embryonic development

A. H&E staining and OCT4 IHC on serial sections from gPAK TGCTs at postnatal day 3 and 6 indicating substantial tumor growth. B. *tdTomato* expression (top) indicating *Stra8-Cre* activity in embryonic germ cells at E12.5 and E18.5 with an absence of expression at E11.5 (N≥6). Expression at P0 was followed by increasingly widespread expression at P3. Brightfield images or DAPI counterstaining are shown below. Scale bars represent 100 μm (A) or 75 μm (B). C. Images from a TGCT identified in a P0 gPAK, *tdTomato*-positive mouse. Whole mount and histological images are all of the same sample. Black and white arrows point to neoplasms identified by *tdTomato* expression in the merged whole mount image and the corresponding images of H&E-stained sections. D-F. Serial-sectioned TGCTs from 10-day (D,F) or 14-day (E) old gPAK mice stained for γH2AX and OCT4. γH2AX is not present in early-stage gPAK TGCT cells expressing OCT4 but is evident in adjacent meiotic germ cells. Scale bar represents 200 μm (D,E) or 100 μm (F).

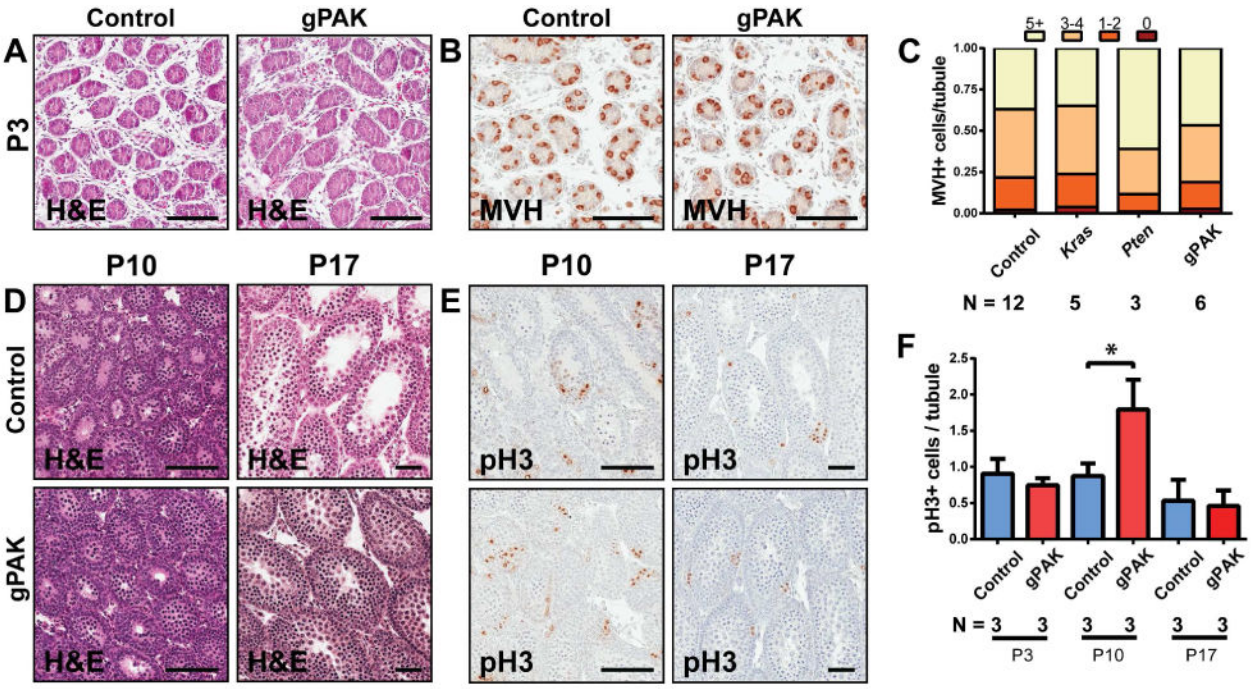

Figure 4. gPAK testes exhibit increased cellularity and phospho-histone H3-positive cells in early postnatal life

A-C. Comparable numbers of germ cells in gPAK and control testes at P3 as shown by staining with H&E (A) or for the germ cell marker MVH (B; quantified for all genotypes in C). D-E. H&E (D) and pH3 IHC staining (E,F) of P10 and P17 control and gPAK testes indicating increased cellularity in the seminiferous tubules of gPAK mice. Increased numbers of mitotic cells, shown by pH3 staining, were detected in gPAK mice relative to controls at P10 (mean +/- SD; Student's T-Test; p=0.045), but not P17. Scale bars represent 100 μm.

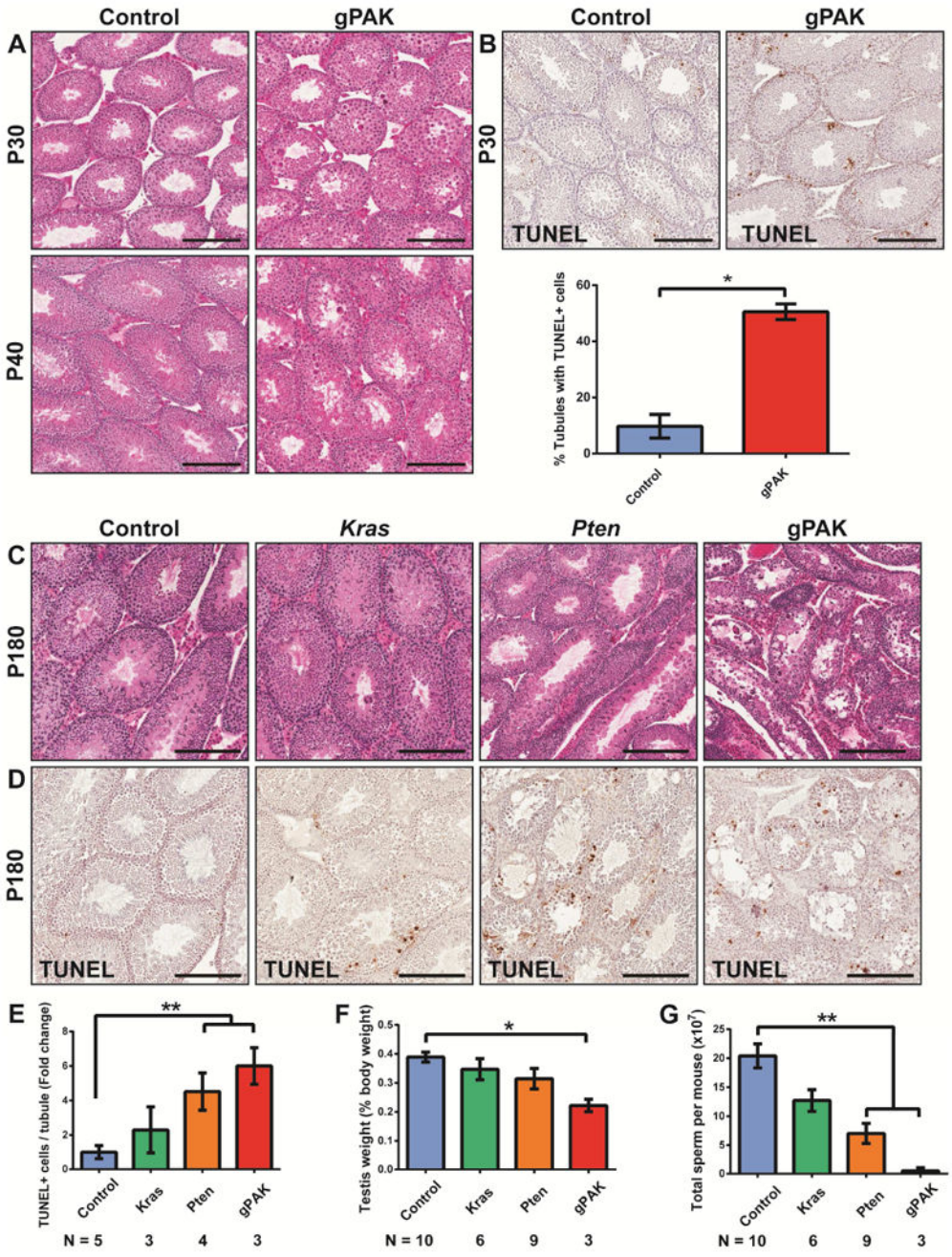

Figure 5. *Pten*/*Kras* targeting in postnatal germ cells is associated with dysplastic histological changes, reduced testis size, and reduced sperm counts in non-tumor-bearing mice

A. H&E staining of P30 and P40 gPAK testes indicates increased germ cell abnormalities compared to controls. B. gPAK testes exhibit significantly increased apoptosis compared to controls (N=3 per group, Student's T-test; $p<0.005$). C-E. 6-month old gPAK mice exhibit significant dysplastic changes in the testis and loss of sperm production. C,D. H&E and TUNEL staining indicating significant vacuolization, increased presence of multinucleate spermatid giant cells and pyknotic nuclei, decreased tubule diameter, and increased apoptosis in gPAK and *Pten* mutants (quantified in E; mean +/- SD; Student's T-Test;

p=0.002; p=0.01 respectively). F,G. Graphical representations of testis weights (F) and sperm counts (G) from 6-month old mice of the indicated genotypes (mean +/- SEM; *p<0.005, Student's T-test; **p<0.001, Tukey-Kramer HSD test). Scale bars represent 200 μm.

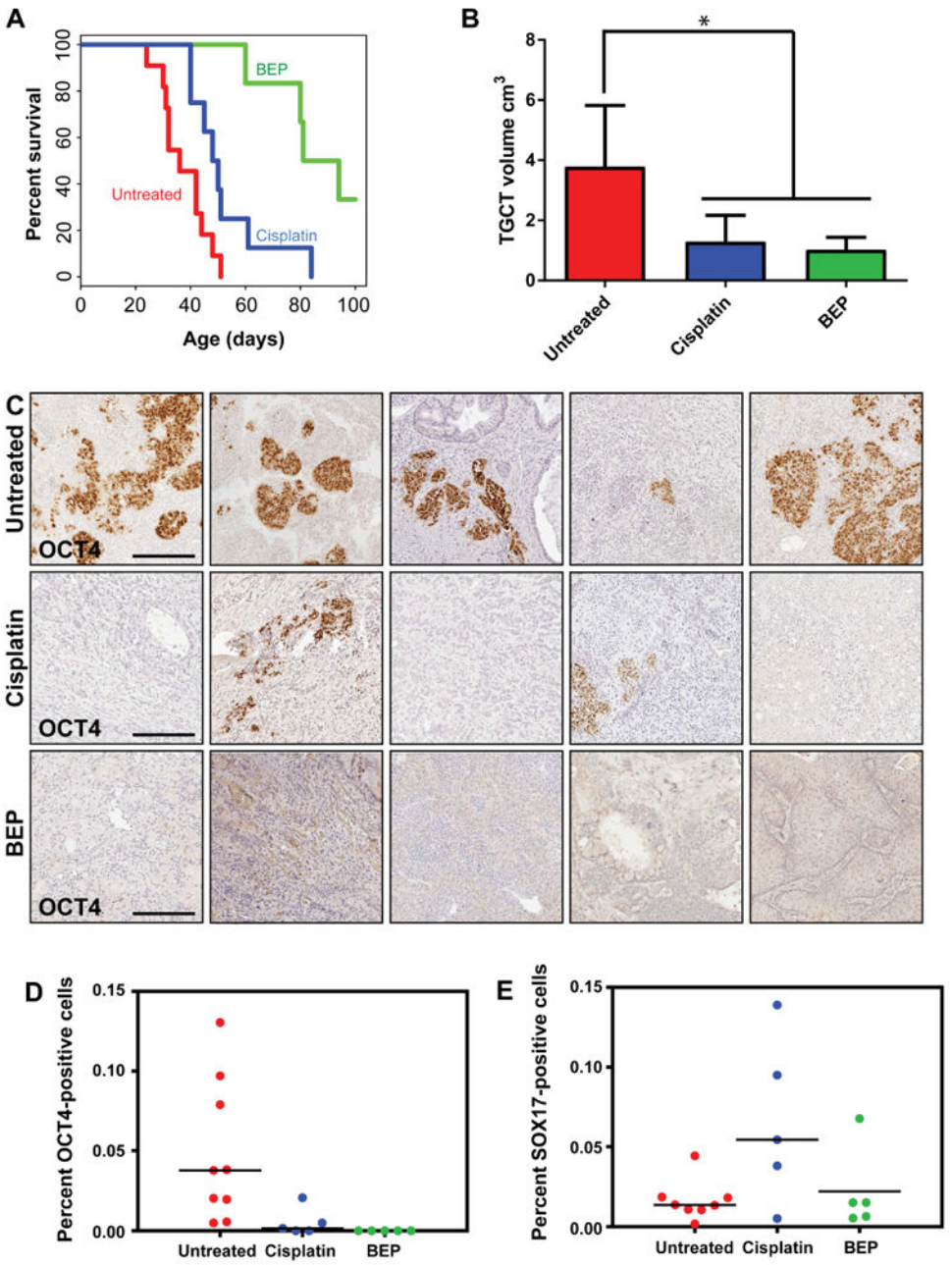

Figure 6. Genotoxic chemotherapeutic treatment of gPAK mice prolongs survival and selectively depletes OCT4^{+} cells

A. Kaplan-Meier survival curve indicating prolonged survival of gPAK mice following two intraperitoneal doses of 6 mg/kg cisplatin, or a 4 week BEP regiment. The median survival of cisplatin-treated mice was 13 days greater than in untreated mice (N=10 and 8, respectively; log-rank test; $p<0.02$) and 58 days longer in BEP-treated mice than in untreated mice (N=5; log-rank test; $p<0.0005$). B. Primary tumor volume measured at endpoint was significantly reduced in cisplatin-treated (N=9; mean +/- SEM; Student's T-Test; $p=0.007$) and BEP-treated (N=4; mean +/- SEM; Student's T-Test; $p<0.002$) gPAK mice. C. OCT4

IHC on primary TGCTs from untreated, cisplatin-treated, and BEP-treated gPAK mice. Scale bars represent 200 μm. D. Quantification of $OCT4^{+}$ (Student's T-Test; p=0.02 (cisplatin); p<0.002 (BEP)) and E. SOX17-positive (Student's T-Test; p=0.098 (cisplatin); p=0.67 (BEP)) cells in untreated, cisplatin-treated, and BEP-treated gPAK TGCTs, counted using Image-J. See Fig. S6 for SOX17 images.

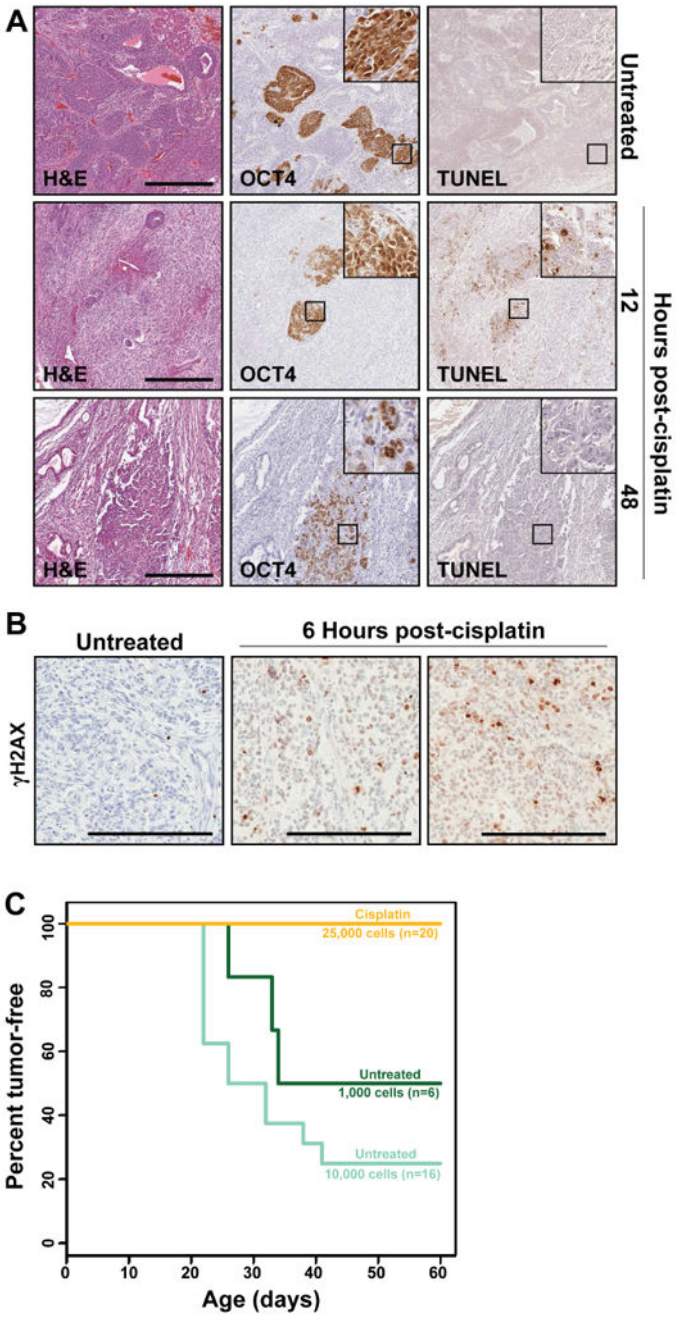

Figure 7. Cisplatin treatment of gPAK TGCTs induces apoptosis of OCT4$^+$ cells and reduces tumorigenicity of transplanted tumor cells

A. TGCT-bearing gPAK mice were euthanized either without treatment, or 12 or 48 hrs following a single 6 mg/kg cisplatin dose. Serial sections of fixed tumors were stained with H&E, OCT4, or TUNEL, revealing apoptosis in EC cells at 12 hours post treatment. B. Tissue sections from additional mice were stained for γH2AX. Robust γH2AX signal was apparent at 6 hrs post-cisplatin treatment. C. Portions of gPAK primary TGCTs, from either untreated mice or mice euthanized 48 hrs post-cisplatin treatment, were disaggregated and the indicated number of cells were injected subcutaneously into NOD.CB17-Prkdcscid/J

mice (see Table S5 for tumor incidence, primary tumor source, OCT4 staining results). Kaplan-Meier tumor-free survival curve showing 25,000 post-treated cells (n=20) did not form tumors at injection sites while 75% of sites injected with 10,000 untreated cells (n=16) formed tumors that reached approximately 200 mm^3 3-5 weeks post-transplant (log-rank test $p<0.005$). Scale bars represent 400 μm.